Petroleum Technology Development Journal

Evaluation of Steady and Unsteady Flow Phenomena Using Computational Fluid Dynamics (CFD) Modelling Methodology in Circulating Fluidised Bed (CFB)/Fluid Catalytic Cracking (FCC) Reactor Systems.

By

M. N. Idris [***], T. Mahmud[**] and B. M. Gibbs[*]

Abstract

The simulation framework was developed from the licensed computational fluid dynamics (CFD15) software to simulate the hydrodynamics of gas-solid flow in CFB/FCC riser reactors. The predictions from the commercial CFD code (CFX and fluent) were based on the Eulerian-Eulerian multiphase model using k-ε model. A validation using published experimental data from the open literature was conducted. The flow model is based on an Eulerian-Eulerian description of the phases where the kinetic theory for granular flow (KTGF) forms the basis for the turbulence modelling in the solid phases. In addition, for constant diametre and particle density, better understanding of the hydrodynamics of the gas-solid flow, under various loading of gas and solid flux were achieved. Within the limit of the computational error, it was found that the choice of the ANSYS Fluent solver provide the best understanding on the gas-solid hydrodynamics in CFB/FCC riser systems. In addition, the availability of transport KTGF in Fluent solver was a focus reason why the concluded choices of establishing a better understanding of the gas-solid hydrodynamics in riser reactors were deduced.

Keywords*: CFD, Hydrodynamic, Multiphase gas-solids, CFB, FCC riser and Simulation*

1. Introduction

Fluid catalytic cracking units (FCC) is one of the most viable, expensive and important process in the modern refineries around the globe. This cracking of heavy petroleum fractions ($C_7H_{15}.C_{15}H_{30}.C_7H_{15}$) process into straight-run atmospheric gas oils, vacuum gas oils, atmospheric residues, and recovered from other units of refinery operations is carried out in a short-contact-time riser reactor. The feed into the FCC unit are from the crude oil distillations unit (CDU), vacuum distillation unit (VDU) residue, and refined into economic and lower molecule-weight products, such as high-octane gasoline, diesel, light fuel oils and olefin-rich light gases, etc., in the presence of a FCC catalyst of average particle size about 70μm[1, 2]. Recently, renowned researchers reported some experimental studies on hydrodynamics in riser system.

[*]Energy Resources and Research Institute, SPEME, University of Leeds, United Kingdom
**Institute of Particle Science and Engineering, SPEME, University of Leeds, United Kingdom
[***]Department of Chemical Engineering, University of Maiduguri, Born State, Nigeria.

[1] David S., Jones J., and Peter P. Pujado (2006), *'Handbook of Petroleum Processing'* (First Ed.). Springer. ISBN 1-4020-2819-9

[2] Speight J. G (2006), '*Petroleum Chemistry and Refining'*, Heinz Heinemann Book Company, pp. 39 - 54

Amongst are[3] where a non-isokinetic sampling technique were used to explore the flow structure at five angular and three axial positions along the riser of height 6.2 m and diametre 0.152 m, using Geldart B particle of density 2646 kg/m^3 and particle diametre of 200 µm. They found some distinctive features of peaks located around the radial profile position r/R_T = ±0.6. Some researchers attributed this peculiarity to the behaviour of Geldart A power.

They reported a good symmetric profile of solid flux around the riser over a wide range of operating conditions, non-symmetric profiles were also observed.[4] reported that the flow development in the riser centre is almost instant with the solids holdup remaining constant and low, and particle velocity along the length of 15.1 m riser and diametre 0.1 m and found that the particle flow firstly developed from the riser centre, and then toward the wall, since the riser height is an important factor for the design of CFBs. Equally they report that, increasing the solid circulating rate significantly slows down the flow development process, while increase in the superficial gas velocity accelerates the flow process. More so, in the wall region, the flow development is significantly slower, with the solids holdup near the wall decreasing slowly towards the riser top. In addition, they state that increasing the superficial gas velocity lengthens the fully developed region, while the flow development becomes remarkably slower with the increase of solids circulation rate at a constant U_g. CFD is a state-of-the-art numerical technique for modelling fluid flow, heat transfer, and chemical reactions in complex geometries. In modelling FCC particles, known as Geldart's group A particles in riser reactors, we know that the particles are slightly cohesive and have a wide range of particle size averaging 70 µm. Recently,[5] investigation on the hydrodynamics and mixing behaviours in a riser-downer-coupling reactor was proposed for the fluid catalytic cracking (FCC) process. They proposed a cluster-based approach (CBA) and also observe a core-annular flow structure in risers in their simulation.

The work of [6] and[7] was on the simulations that support the idea of average drag coefficient is an important factor for the two-fluid model and suggest that the energy-minimisation multiscale (EMMS) approach could be used as a kind of multiscale closure law for drag coefficient.[8] uses the experimental results from a high-density circulating fluidized bed (HDCFB) riser to develop a closure models for the drag coefficient and the gas-solid mixture viscosity, using a 3D cylindrical vessel of 0.104 m diametre and 1.0 m in length. The particle average size is between 69.8 – 100 µm of density 1310 kg/m^3. Their model predicts a rapid increase in both viscosity and drag associated with high solids concentrations near the riser wall.[9] relate that turbulent fluidisation regime is characterised by the co-existence of a dense, bottom region and a dilute, top bed.

---

[3] Salvaterra A, Gildert D and Ocone R (2005), '*Solid Flux in a Circulating Fluidised Bed Riser'*, Journal of Institute of Chemical Engineers, **83**(A1): pp. 24 – 29

[4] Huang, W., Yan, A., and Zhu, J., (2007), *'Hydrodynamics and Flow Development in a 15.1m Circulating Fluidised Bed Riser'*, Chem. Eng. Techno. **30**, No. 4, pp. 460 – 466

[5] Idris M. N. (2010), *'Hydrodynamics and Process Modelling of Fluid Catalytic Cracking Reactors'*, a PhD Thesis published the University of Leeds British Library Ethos, United Kingdom.

[6] Lu, J., (2005), *'Particle and gas dynamics of high density CFBs'*. PhD. Thesis, the University of British Columbia, Vancouver, BC.

[7]Yang et al (2004) Yang, N., Wang, W., Ge, W., Wang, L., Li. J., (2004), *'Simulation of Heterogeneous Structure in a Circulating Fluidized-Bed Riser by Combining the Two-Fluid Model with EMMS Approach'*. Industrial and Engineering Chemistry Research **43**, pp. 5548 - 5561.

[8] Wang W, Lu B, Wang W, Li J, Wang X, Gao S, Lu W, Xu Y and Long J., (2006), *'Multi-scale CFD Simulation of Gas–Solid Flow in MIP Reactors with a Structure-Dependent Drag Model'*, Chemical Engineering Science Volume 62, Issues 18-20, September-October 2007, pp. 5487 - 5494.

[9] Pugsley T, Steward F.R., and Cruz E., (2006), *'New Closure Models for CFD Modelling of High-Density Circulating Fluidised Beds'*, Powder Technology **169**, pp. 115 – 122.

Most previous studies address laminar flow situations, using coarse grids, although there are couple of investigations that addresses turbulent model. However, much work still needs to be done, especially that associated with the turbulent flow, kinetic and momentum interactions, and transient nature of the FCC reaction processes. The significance of this research is for better understanding of the interaction of CFB/FCC riser gas-solid hydrodynamics, heat transfer and cracking reaction kinetics. In this study, a replica-straight FCC riser reactor was developed and serial steps were used as follows: (a) steady state non-KTGF (simple Miller Gidaspow) model, (b) steady state KTGF, and (c) algebraic-KTGF modelling approach.

2. Experimental Description: CFD Boundary Domain

The adopted experimental setup used in this paper is based on the study conducted as shown in Figure 1. The experiment was conducted with a riser of 15.1m height and 0.10m diameter. The solids used in the riser setup were FCC particles and had a mean particle diameter of 67μm and density 1500kg/m^3. Ideal air near ambient conditions was the gas used in these experiments. The setup on Figure 1 is much longer than many other research works when compared. The solids flow from the storage tank into the riser distributor region where the solids are fluidised by the auxiliary air. The main air enters through a series of 13mm outer diameter tubes extending 0.30m into the riser bottom to carry the gas-solids suspension up the riser and through a smooth exit into the primary cyclone. The bottom of the cyclone connects to the distributor of the downer. The riser air from the cyclone is sent through a proper cleaning channel before exhausted to the atmosphere.

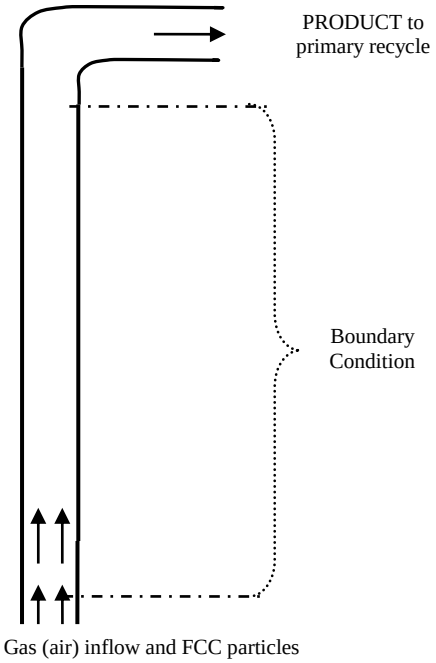

Figure 1: Process flow of CFB/FCC pilot plant

Reflective-type fibre optic concentration probe were used to determine solids concentration.

3. Modelling Description

An Eulerian-Eulerian model with the kinetic theory of granular flow was used to model the hydrodynamics of the gas-solid flow in the CFB/FCC riser system. One set of the mass and momentum equations were solved for each phase, where the momentum equations were linked by an interphase exchange term.

3.1 Continuity Equations (Conservation of Mass)

The Reynolds-averaged continuity equations for the gas and solid phases are given by[10] [11]:

$$\frac{\partial}{\partial t}\left(\varepsilon_g \rho_g\right) + \nabla.\left(\varepsilon_g \rho_g \vec{v}_g\right) = 0 \tag{1}$$

where ρ_g and $\vec{v}_g$ are the gas density and gas velocity vector, respectively. The first term on left hand side is the transient and the second is the convective. The solid phase continuity equation is [11]:

$$\frac{\partial}{\partial t}\left(\varepsilon_s \rho_s\right) + \nabla.\left(\varepsilon_s \rho_s \vec{v}_s\right) = 0 \tag{2}$$

Where ρ_s and $\vec{v}_s$ are the solid density and solid velocity vector, respectively, and ε_s is the volume fraction [11].

3.2 Momentum Conservation Equations

The Reynolds-averaged momentum conservation for the gas phase is described by [12]:

$$\frac{\partial}{\partial t}\left(\varepsilon_g \rho_g \vec{v}_g\right) + \nabla.\left(\varepsilon_g \rho_g \vec{v}_g^{\,2}\right) = -\varepsilon_g \nabla p + \nabla \bar{\bar{\tau}}_g + \varepsilon_g \rho_g \vec{g} + K_{gs}\left(\vec{v}_g - \vec{v}_s\right) \tag{3}$$

Transient — Convective — Pressure — Stress — Body force — Interphase force exchange

The momentum conservation for the solid phase is described by[11]:

$$\frac{\partial}{\partial t}\left(\varepsilon_s \rho_s \vec{v}_s\right) + \nabla.\left(\varepsilon_s \rho_s \vec{v}_s^{\,2}\right) = -\varepsilon_s \nabla p + \nabla \bar{\bar{\tau}}_s + \varepsilon_s \rho_g \vec{g} + K_{gs}\left(\vec{v}_s - \vec{v}_g\right) \tag{4}$$

Transient — Convective — Pressure — Stress — Body force — Interphase force exchange

where p is the pressure, ε is the volume fraction, g is the gravitational acceleration, K_{gs} is the gas-solid momentum exchange coefficient and $\bar{\bar{\tau}}_{\varphi(g,s)}$ are the stress tensors, respectively. The sum volume of gas and solid particle is equal to unity.

The momentum exchange between the solid and gas phase is expressed by the drag force, which is represented by an interphase exchange coefficient and the stress tensors $\Delta\bar{\bar{\tau}}_g$ and $\Delta\bar{\bar{\tau}}_s$. Several drag models exits for the gas-solid interphase exchange coefficient K_{gs}, including the drag laws of Symlal O'Brien, Arastoopour, and Gidaspow [12].

$$\varepsilon_g + \varepsilon_s = 1 \tag{5}$$

---

[10] Jiradilok V, Gidaspow D, Damronglerd S, Koves W. J, and Mostofi R (2006), *'Kinetic theory based CFD Simulation of Turbulent Fluidisation of FCC Particles in a Riser'*, Chemical Engineering Science **61**: pp. 5544 – 5559.

[11] ANSYS CFX (2015), '*Solver Theory Guide. ANSYS CFX Release 15.0*': 2015 ANSYS Europe, Ltd

[12] Gidaspow, D., R. Bezburuah, and J. Ding., (1990), *'Hydrodynamics of Circulating Fluidized Beds, Kinetic Theory Approach*'. *In* Fluidization VII, Proceedings of the 7th Engineering Foundation Conference on Fluidization, pp. 75 - 82.

3.3 Conservation of Solid Phase Fluctuating Kinetic Energy: Granular Temperature, Θ_s .based on Transport Model Equation in Fluent

The granular temperature, $\boldsymbol{\Theta}_s$ describe the particle-particle interaction compared to classical two-fluid model. In this case, the gas-solid hydrodynamic profiles with incorporation of the KTGF, the predictions under algebraic relations, which depend on $\boldsymbol{\Theta}_s$. That is, in a simple term:

$$\boldsymbol{\mu}_s = \sqrt{\boldsymbol{\Theta}_s}\,, \qquad \boldsymbol{\Theta}_s \text{ depends on } \left(\frac{\partial \boldsymbol{u}^i}{\partial \boldsymbol{x}^j}\right)^2 \tag{6}$$

Equation (6) shows that, the granular temperature, $\boldsymbol{\Theta}_s$, depends on the square of the shear viscosity of the solid particles. The algebraic $\boldsymbol{\mu}_s \propto \left(\frac{\partial \boldsymbol{u}^i}{\partial \boldsymbol{x}^j}\right)^2$ will predict a low velocity profiles in ANSYS CFX 11.0 which is not well developed at present.

The kinetic theory of granular flow (KTGF) is an extension of the classical kinetic theory of dense gases. KTGF is a tool developed from the kinetic theory of gases to describe the fluctuation velocity of fluid flow in solid phase. Previous work has shown that the KTGF can be used to describe the particle motion in a fluidized bed due to the inherently random particle movement caused by the fluid mechanics[13] and Gidaspow, et al [14]. The conservation of the fluctuating kinetic energy of moving particles is described as follows in terms of the granular temperature, Θ_s , which is derived from the kinetic theory of granular flow and is represented by ANSYS Fluent 2015:

$$\frac{2}{3}\left[\frac{\partial}{\partial t}\left(\rho_s \varepsilon_s \Theta_s\right) + \nabla.\left(\rho_s \varepsilon_s \vec{v}_s \Theta_s\right)\right] = \left(-p_s \bar{\bar{I}} + \bar{\bar{\tau}}_s\right) : \nabla \vec{v}_s + \nabla \cdot \left(k_{\Theta s} \nabla \Theta_s\right) - \gamma_{\Theta s} + \phi_{gs} \tag{7}$$

In equation (6), the first term on the right-hand side is the production of fluctuating energy by the effective shear stresses, the second term is the diffusion due to the gradient of Θ_s , and the third term is the dissipation due to the inelastic collision of particles. The pressure P_s , are modelled as a function of Θ_s [12].

To solve Equation (6), we need to specify the collisional energy dissipation, $\gamma_{\Theta s}$, due to inelastic collision of particles and the granular conductivity, $k_{\Theta s}$.

The transport model equation should have a better prediction when compared with algebraic model equation. The reason is that, the equations incorporate a real translation of the fluctuation in the multiphase flow situations.

For turbulent flows, the instantaneous equations are averaged leading to additional terms. In the most general kinetic theory models, the granular temperature is derived from a differential transport equation of Θ_s as represented in Equation (6). However, these ignored terms in

---

[13] Gidaspow, D., Jonghwun, J., Singh, R. K., (2004), '*Hydrodynamics of Fluidization using Kinetic Theory*': an emerging paradigm 2002 Flour-Daniel lecture. Powder Technology 148, pp. 123 – 141

[14] Gidaspow D., Jiradilok V., Breault R. W. (2006), '*Computation of Gas and Solid Dispersion Coefficients in Turbulent Risers and Bubbling Beds,'* Chemical Engineering Science Volume 62, Issue 13, pp. 3397 – 3409

algebraic approach are incorporated in the transport modelling approach. The advantages of using transport model, is that, it gives a better prediction when compared with that of algebraic model equation [11, 14].

The governing equations for the gas and solid flow are solved, using the finite volume method, including the continuity and momentum equations, and constitutive equations, and in addition, the kinetic fluctuation energy, etc.

3.4 Constitutive Equations

The constitutive model equations for both the gas and solid phase stress tensors are described below:

The solid phase stress model is represented by Equation (8) as:

$$\vec{\tau}_s = -\frac{\pi}{6}\sqrt{3}\phi\frac{\varepsilon_s}{\varepsilon_{s,\max}}\rho_s g_0 \sqrt{\Theta_s}\vec{U}_{s,\parallel} \quad (8)$$

Stress Tensor

Where $\vec{U}_{s,\parallel}$ is the particles slip velocity parallel to the wall, ϕ is the specularity coefficient between the particle and the wall, $\alpha_{s,\max}$ is the volume fraction for the particles at maximum packing, and g_0 is the radial distribution function that is model dependent[15].

The solid Pressure, p_s :

The solid phase pressure, p_s , is described in terms of granular temperature as (ANSYS CFX 2006):

$$p_s = \varepsilon_s\rho_s\Theta_s\left[1+2g_0\varepsilon_s(1+e)\right] \quad (9)$$

where e is the restitution coefficient, ρ_s is the solid density, Θ_s is the granular temperature, g_0 is the radial distribution function, and ε_s is the solid volume fraction.

The Radial Distribution Function

The radial distribution is a correction factor (non-dimensional distance between spheres) that modifies the probability of a single particle touching another particle in the solid phase, that is, the collisions possibility between particle grains when the granular phase becomes dense (ANSYS CFD 2006):

$$g_{o,ss} = \left[1-\left(\frac{\varepsilon_s}{\varepsilon_{s,\max}}\right)^{1/3}\right]^{-1} \quad (10)$$

The collision dissipation of solid fluctuating energy is also represented using granular temperature as [16]:

[15] ANSYS FLUENT (2015), '*Solver Theory Guide. ANSYS FLUENT Release 15.0'*: 2015 ANSYS Europe, Ltd

The collision dissipation of solid fluctuating energy:

$$\gamma_{\Theta s} = \frac{12(1-e_{ss}^2)g_{0,ss}}{d_s\sqrt{\pi}}\rho_s\varepsilon_s^2\Theta_s^{3/2} \tag{11}$$

From the ANSYS Fluent solver, the details of the solid phase shear viscosity and bulk viscosity are represented as follows:

Solid Phase Shear Viscosity
The KTGF depends on the granular temperature, which is a function of the solid phase shear viscosity is represented in Equation (12). That is:

$$\mu_s = \frac{4}{5}\varepsilon_s^2\rho_s d_p g_{0,ss}(1+e)\sqrt{\frac{\Theta}{\pi}} + \frac{5\sqrt{\pi}}{48}\frac{\rho_s d_p}{(1+e)g_{0,ss}}\left(1+\frac{4}{5}(1+e)g_{0,ss}\varepsilon_s\right)^2\sqrt{\Theta} \tag{12}$$

where e is the restitution coefficient.

The Solid Phase Bulk Viscosity, ξ_s [12]:

$$\xi_s = \frac{4}{3}\varepsilon_s\rho_s d g_0(1+e)\sqrt{\frac{\Theta_s}{\pi}} \tag{13}$$

Exchange of the Fluctuating Energy between Gas and Solid (i.e. the Transfer of Kinetic Energy) is given as (ANSYS CFD 2006):

$$\phi_{gs} = -3\cdot K_{gs}\cdot\Theta_s \tag{14}$$

There are several *drag laws, which* are available in CFD modelling. This includes the Gidaspow, Arastoopour, Syamlal and O'Brien, Schiller Naumann model etc. In this research studies, the Gidaspow-drag correlations was applied because it is a better use for large scale and large cell sizes as applicable in the FCC industries.

The Gidaspow Drag Model:
The gas-solid interphase exchange coefficient is given as:

$$\text{For } \alpha_g > 0.8:\ K_{gs} = \frac{3}{4}\cdot C_D\cdot\frac{\varepsilon_s\cdot\varepsilon_g\cdot\rho_g\cdot\left|\vec{v}_s-\vec{v}_g\right|}{d_s}\cdot\varepsilon_g^{-2.65} \tag{15}$$

C_D, the drag coefficient, is expressed as

$$C_D = \frac{24}{\varepsilon_g\cdot \mathrm{Re}_s}\cdot\left[1+0.15\cdot(\varepsilon_g\cdot\mathrm{Re}_s)^{0.687}\right] \tag{16}$$

$$\text{Also for } \alpha_g \le 0.8:\ K_{gs} = 150\frac{\varepsilon_s^2\cdot\mu_g}{\varepsilon_g\cdot d_s^2} + 1.75\cdot\frac{\varepsilon_s\cdot\varepsilon_g\cdot\rho_g\cdot\left|\vec{v}_s-\vec{v}_g\right|}{d_s} \tag{17}$$

In the course of establishing the potentials and limitations of the CFD model, the model was evaluated for different operating conditions ranging from the low to slightly high-density flow. The same modelling parameters were used for all the cases with varying only the superficial gas velocity, U_g, and/or solid mass flux, G_s, to match the experimental operating conditions. A summary of the various operating conditions of different cases are provided in Table 1.

Table 1 Summary of operating conditions with corresponding numerical values

Operating conditions	(Huang et al., 2007) [16]				(Van engelandt et al., 2007) [17]		
	Case 1.1	**Case 1.2**	**Case 1.3**	**Case 1.4**	**Case 2.1**	**Case 2.2**	**Case 2.3**
G_s (kg/m^{2}s)	100	50	100	200	0.5	3	4.5
U_g (m/S)	3.5	5.5	5.5	8.1	5.3	6.4	7.4

3.5 Solution procedure

A commercial ANSYS CFD package (CFX and Fluent Inc., V6.2) was used to provide a numerical solution for the governing equation. In this study, the simulation modelling was performed progressively, with initial consideration of without-KTGF (simple Miller Gidaspow), and then inclusion of KTGF (in both ***steady*** and ***transient*** calculations) based on algebraic model equation in CFX. For the steady state calculation without-KTGF, the solver was run maximum iterations of 3000 – 5000, using automatic time scale control on a convergence target of 0.010 using Advective high-resolution scheme. While for the transient simulation, total time duration of 2s, 5*s*, 10s, 15s and 20 s were consecutively run at each simulation. Various time steps were run in each case, and to confirm the quality of the result, a comparison of the input data with predicted values was carried out.

The time averaged distributions of flow variables were computed and the results from the *5s* time step are almost similar to the rest of the simulation except that of the 2s time step. Therefore, it was concluded that a total time step of 5s is the most realistic value that is suitable in this particular modelling.

A high-resolution advection scheme was used for the turbulent calculations using transient second order backward Euler, and automatic time step initialisation on convergence target of 0.01 and residual criteria of 1.0×10^{-4}. The convection terms were discretised using a high-resolution scheme [12], in order to reduce the numerical diffusion errors. The boundary conditions (at the inlet, outlet, all velocities and volume fractions of gas and solid) were correctly specified, in the solver domain, as shown in Figure 2 - 5.

However, it is difficult to accurately specify the exact inlet conditions at this stage, because of their transient nature. In this study, both gas and solid was introduced at the same inlet point, which differ from the real situation. At the walls, the no-slip boundary condition was specified for both gas and solid phase, and this is not realistic for solid phase particles. The discretised RANS, pressure correction and volume fraction equations, together with the equations for turbulence model quantities, were solved iteratively using KTGF-algebraic model technique in ANSYS CFX-15.0 code. Transient computations were performed using zero initialisation starting from 1.0 - 2.5 s time intervals, that is, the computational domain was empty and there were no gas-solid flow fields at the start of the simulation. A zero initialize for a real time of *5* s, with each step of 10^{-4}s duration was used. To ensure the numerical accuracy and stability, the time step for modelling unsteady state conditions was limited by Courant number was 0.01 and 0.12**,** which is a function of smallest cell dimension and the largest instantaneous velocity. For each time step, a maximum number of coefficient

[16] Huang, W., Yan, A., and Zhu, J. (2007), *'Hydrodynamics and flow development in a 15.1 m circulating fluidised bed riser', Chemical Engineering Technology*, **30(4)**, pp. 460-466

[17] De Wilde J., Van engelandt G., Heynderickx G. J., and Marin G. B (2005), *'Gas-Solids Mixing in the inlet zone of a dilute Circulating Fluidized Bed'*. Science direct Powder Technology Journal pp. 96 - 116

loops of 10 - 100 per step was set with a target value of the normalised residual for each variable was 10^{-4}. For a converged solution, the overall mass conservations for the gas and solid phases were typically within 0.01 and 0.03, respectively. In the research work, a typical computational time for the transient simulation was between 10 – 13 days on the 4.0 GHz computer workstation used. More so, these strategic steps were adopted and applied in both applications of ANSYS CFD (CFX and FLUENT) in this study.

3.5.1 Mesh-Dependency Test in FLUENT solver

The grid independency tests were conducted when the ANSYS FLUENT solvers was used, and are detailed as shown in Figure 2 (a) – (f). In this study, several grids were also put to dependency test, and were also established based on the comparisons of experimental data and modelling predictions of various grids, at various modelling conditions as shown in Figure 2 (a) – (f). After careful assessment with each of the grid, a resolution was arrived at using the grid size 565,520 cells, because the predictions were similar with grids 549,524 cells and 878,469 cells. Although, the grids sizes 565,520 cells and 549,524 cells are very close in size. However, due to simulation time-savings, there was no need using a large grid size 878,469 cells. In these independency tests, the grids 565,520 cells and 878,469 cells show a great overlap, but can easily be noticed clearly with the difference in colour coding. Further effort were made to establish the dependency test further in this case, the predictions of solid holdup at radial position along the FCC riser system were also carried out as shown in Figures 2 (a) – (c). Figure 2 (a) represent the profiles for Case 1.1, (b) for Case 1.2, and (c) for Case 1.3. In this case scenario, it was observed that, there were slight or no much observed differences between the grids sizes 549,524 cells, 565,520 cells and 878,469 cells.

The test for restitution coefficient was equally carried out to further establish the grid dependency test. The detail effects of the restitution coefficient are shown in Figure 2 (c) – (d). In Figure 2 (d), radial positions of 0.95 were used to establish various effect of restitution coefficient with respect to gas-solid hydrodynamic flow along the FCC riser length. In addition, the continuous increase in grid density may lead to slightly better results that are more grid-independent. However, the computational capability currently available is still a restricting factor when using a well refine grid.

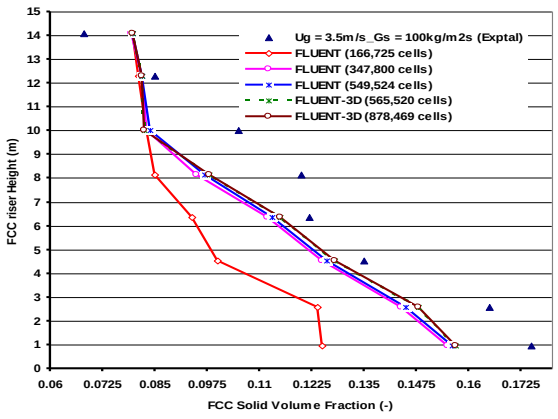

Fig 2 (a): Predicted volume fraction as a function of height, radial axis (r/R) = 0.95 fluent-3D (Case 1.1)

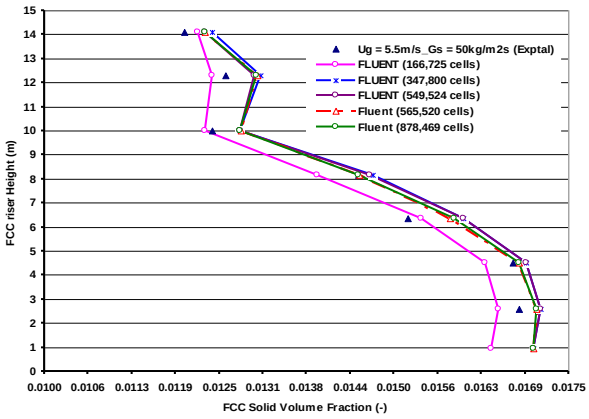

Fig 2(b): Predicted volume fraction as a function of height, radial axis (r/R) in = 0.95 Fluent-3D (Case 1.2)

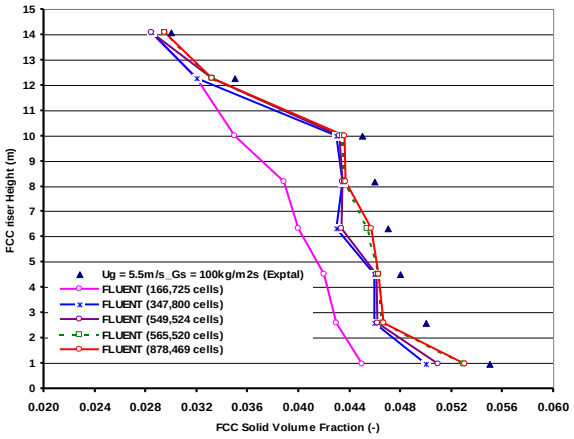

Fig 2(c): Predicted volume fraction as a function of height, radial axis (r/R) = 0.95 fluent-3D (Case 1.3)

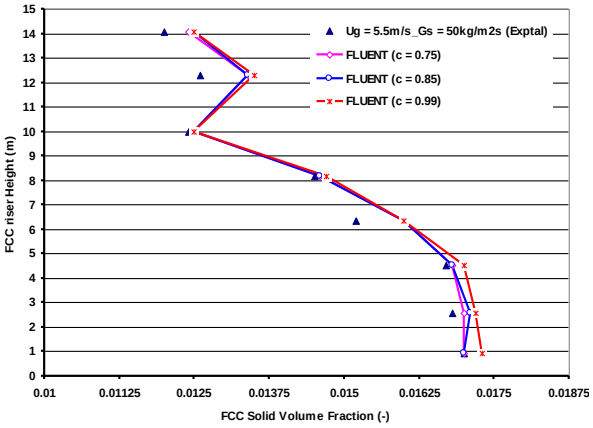

Fig 2(d): Effect of restitution coefficient as a function of height, radial axis (r/R) in = 0.95 Fluent-3D (Case 1.3)

Figure 2: Various predictions for volume fraction as a function of height, radial axis (r/R) = 0.95

In the course of this study, other finer grids of sizes 1,124,475 cells and 1,302,484 cells were generated. The simulation runs were not successful in these cases, due to the limited memory capacity of the workstation. In addition, all the grids used for the simulations carried out in this research work were tested for independency. Figure 3 depicts the various predictions for the FCC particle velocity and solid holdup along the riser axis of the FCC reactor. The grid dependency test of FCC Particle Velocity and solid holdup at various selected plane along the FCC riser reactor were detailed in this figure, where 3(a) represent the FCC Velocity at y = 2.59 m, (b) the Holdup at y = 2.59 m, (c) Velocity at y = 10.0 m, (d) Holdup at y = 10.0 m, (e) Velocity at y = 14.08 m, and (f) Holdup at y = 14.08 m (Straight-Riser pipe). The grid size of 565,520 cells was used in case 1.2 (Huang et al., 2007). The close assessment of these grids gives a clear designation of the choice of the grid size that was used to address the hydrodynamic studies of the gas-solid flow in the FCC riser reactors.

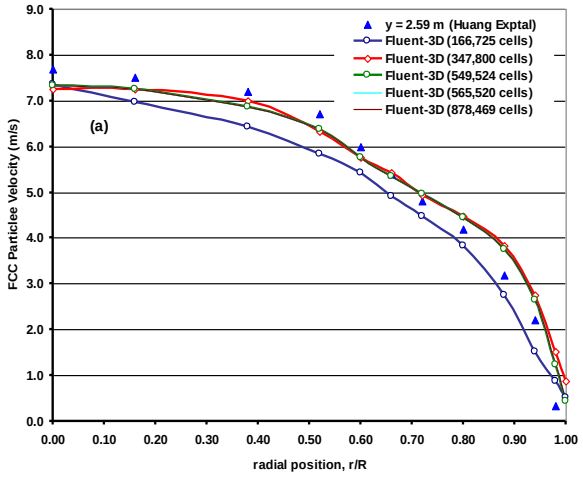

Fig 3(a) Velocity at y = 2.59 m,

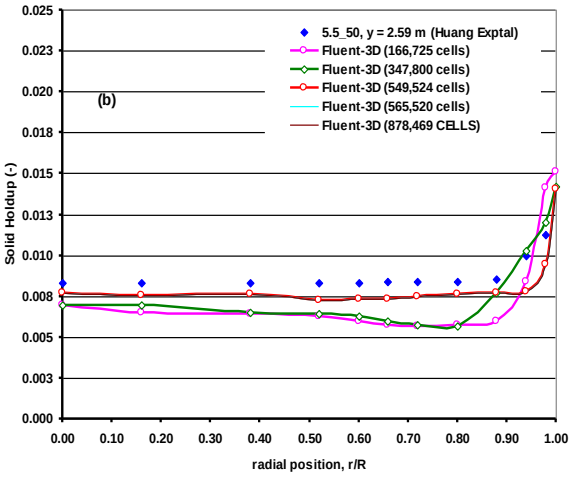

Fig 3(b) Holdup at y = 2.59 m

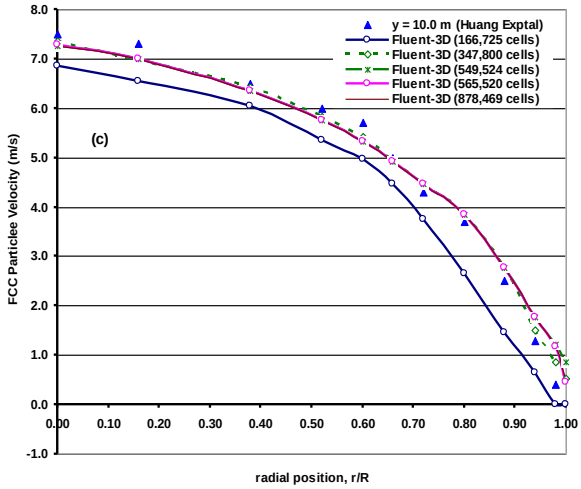

Fig 3(c) Velocity at y = 10.0 m

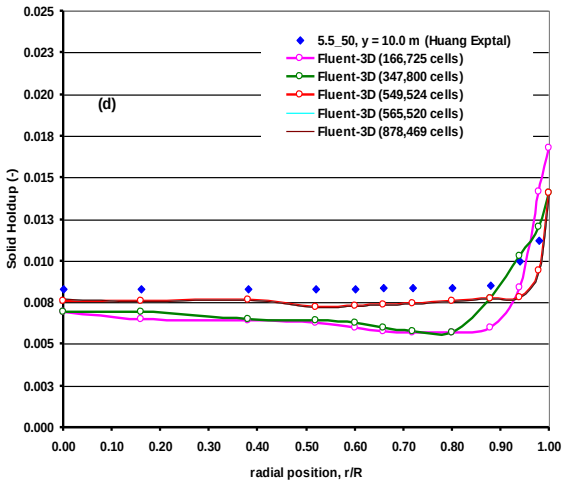

Fig 3(d) Holdup at y = 10.0 m

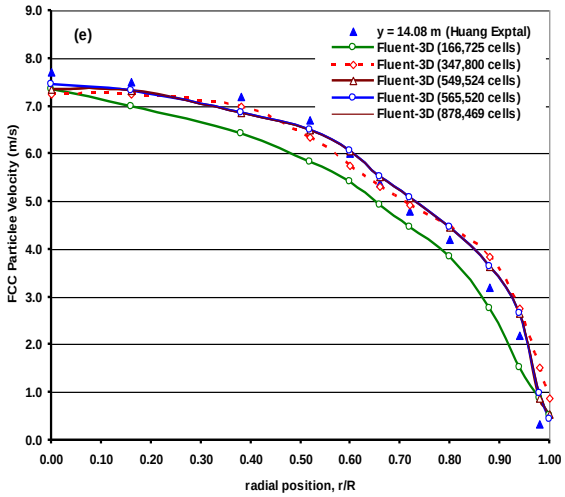

Fig 3(e) Velocity at y = 14.08 m

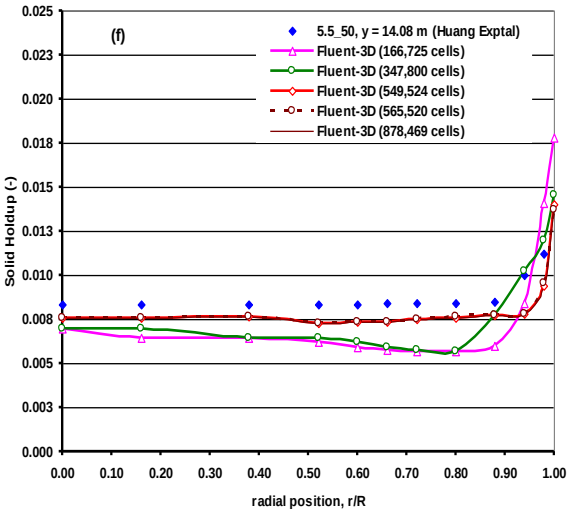

Fig 3(f) Holdup at y = 14.08 m

Figure 3(a) – (f): Grid dependency test of FCC Particle Velocity and solid holdup at various selected plane along the FCC riser reactor: (a) Velocity at y = 2.59 m, (b) Holdup at y = 2.59 m, (c) Velocity at y = 10.0 m, (d) Holdup at y = 10.0 m, (e) Velocity at y = 14.08 m, and (f) Holdup at y = 14.08 m (Straight-Riser pipe). The grid of size 565,520 cells was used case 1.2 (Huang et al., 2007)

3.5.2 Comparison of Restitution Coefficient and Drag Law in CFX and Fluent Solvers in Straight Riser

Figure 4 represents the predictions of FCC solid holdup along the riser length using various restitution coefficients, e (e_1 = 0.75, e_2 = 0.85 and e_3 = 0.99). The choice of using these values was based on the previous studies, where the restitution coefficient, e, between 0.75 – 0.99 had been used. In the Figure 4, it is observed that, the model prediction using e_3 = 0.99 shows a closer agreement with the experimental data reported. This was the very reason, the choice of using the restitution coefficient of 0.99 in this simulation.

Previous experience has shown that, the suitability of various drag laws for turbulent modelling of gas-solid flow in CFB/FCC fluidisation provides some variation in axial particle velocity. However, all of these (Gidaspow, Syamlal-O'Brien and Arastoopour drag model etc.) drag models are good, although they have their various deficiencies [18,19] and[20]. Extensive

details of the various drag law model formulations had previously been discussed in [5]. Based on these reasons, the Gidaspow drag correlation is chosen in this simulation study. Previous studies [13, 14] and [15] have shown that the Gidaspow drag model is good for large-scale industrial process, like CFB/FCC riser reactors of this kind [12].

Figure 4 (a) – (f) represent the grid test carried on the 3-cases (Cases 1.1, 1.2 and 1.3) studying the effect of riser height as a function of solid-holdup (volume fraction) of the FCC riser system, for both the CFX and Fluent solver predictions.

For the case of CFX, in comparing the various prediction of each grid, that is, 133,465 cells, 476,690 cells, 550,250 cells and 738,890 cells, Figure 4 (a), (c) and (e). It is further evidence that, the grids 550,250 cells and 738,890 cells give better agreement with the experimental data. Specifically, for the grid size 133,465 cells the prediction has great discrepancies with respect to experimental data. Therefore, the grid size 133, 465 cells cannot be used in any of this case. This is because it has not satisfied the independency rule for grids in CFD modelling approach. In the same vein for the Fluent, Figure 4 (b), (d) and (f) the grid sizes 166,725 cells, 347,800 cells, 549,524 cells, 565,520 cells and 878,469 cells were tested, because they provide reasonable mesh independent results. However, the grid size 166,725 cells cannot be use too, but the independency test result is not good enough.

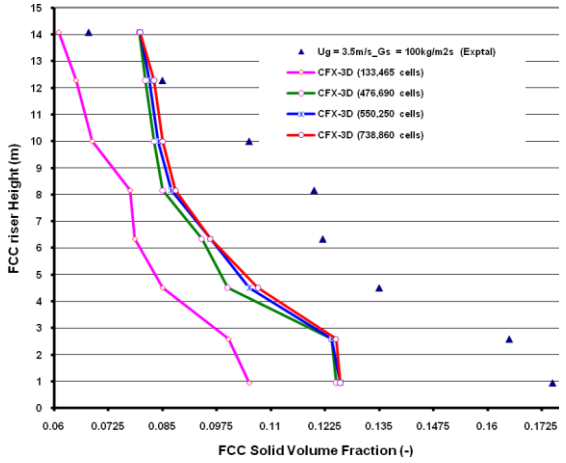

Fig 4 (a): Predicted of FCC volume fraction as a function of height, radial axis (r/R) = 0.95 Fluent-3D (Case 1.1)

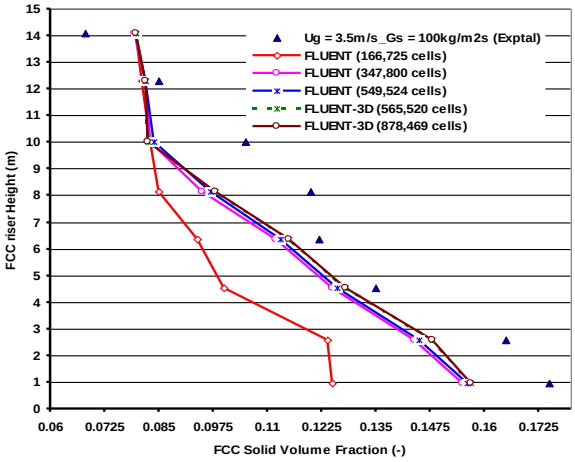

Fig 4 (b): Predicted volume fraction as a function as a function of height, radial axis (r/R) in Fluent-3D(Case 1.1)

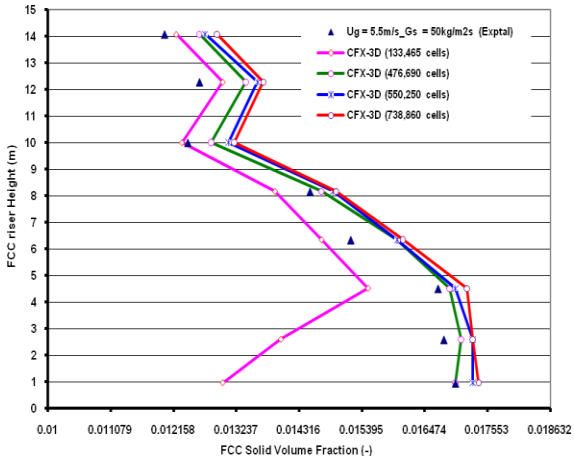

Fig 4 (c): Predicted of FCC volume fraction as a function of height, radial axis (r/R) = 0.95 Fluent-3D (Case 1.2)

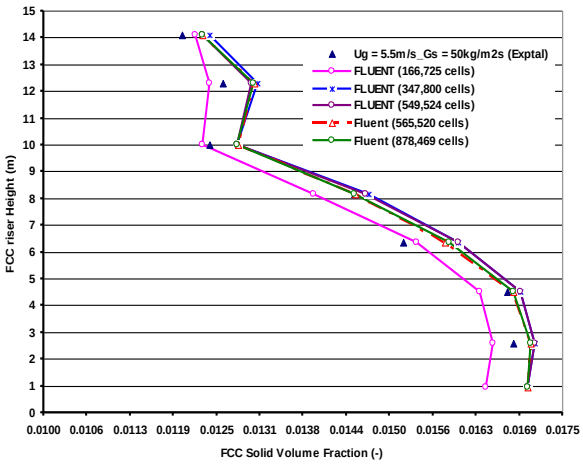

Fig 4 (d): Predicted volume fraction as a function as a function of height, radial axis (r/R) in Fluent-3D(Case 1.2)

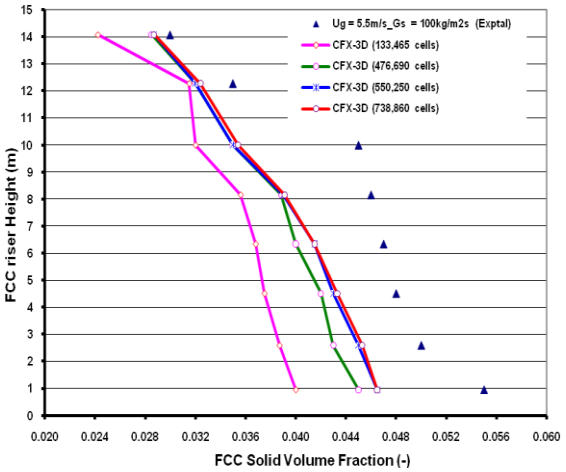

Fig 4 (e): Predicted of FCC volume fraction as a function of height, radial axis (r/R) = 0.95 Fluent-3D (Case 1.3)

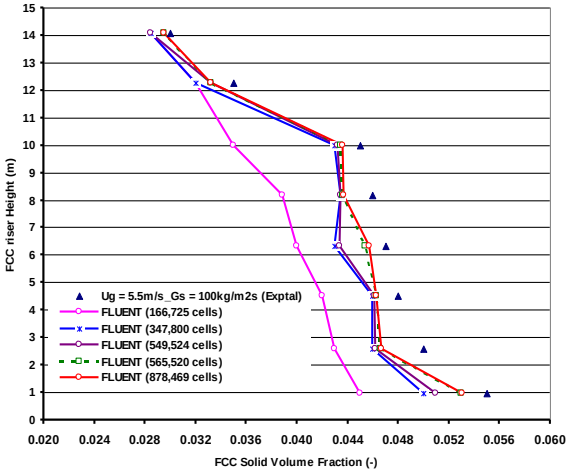

Fig 4 (f): Predicted volume fraction as a function as a function of height, radial axis (r/R) in Fluent-3D(Case 1.3)

Figure 5(a) and 5 (b) represents the effect of restitution coefficient as a function of height for both the CFX and Fluent predictions respectively. In the comparison of the two solvers, it is observed that the fluent solver equally give a better predictions.

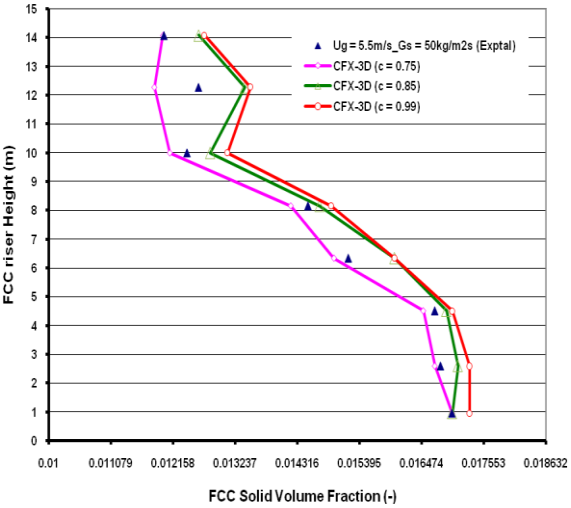

Fig 5 (a): Effect of restitution coefficient as a function of height, radial axis (r/R) = 0.95 CFX-3D (Case 1.2)

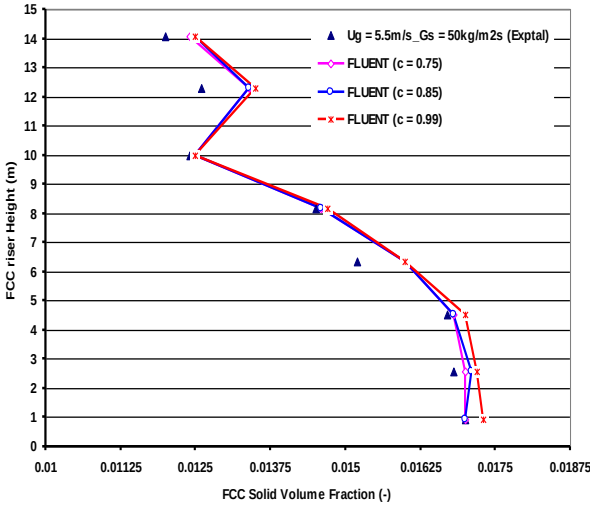

Fig 5 (b): Effect of restitution coefficient as a function as a function of height, radial axis (r/R) in Fluent-3D(Case 1.2)

In the course of this study, other finer grids of sizes 1,124,475 cells and 1,302,484 cells were generated. The simulation runs were not successful in these cases, due to the limited memory capacity of the workstation. In addition, all the grids used for the simulations carried out in this research work were tested for independency.

4 Results and discussions

Table 2 represents the flow parameters used in the simulation. Tables 3 represent a comparison of the input parameters outlet predicted values for the steady state simulation. While Table 4, depicts the transient modelling calculation for this case. From these tables, it was observed that, there are good agreement between the input data for both the gas and the FCC solid particles, when compared with the predicted outflow from the simulation.

Table 2 Flow parameters used in the CFD numerical simulation (Huang et al., 2007)[16]

Parameters	Description	Input values
ρ_g (kg/m^3)	Gas density	1.185
ρ_s (kg/m^3)	Solid density	1500
μ_g (kg/ms)	Gas dynamic viscosity	1.831×10^{-5}
d_p (μm)	Particle diameter	67
r_{coeff} (dimensionless)	Particle-particle restitution coefficient	0.99
e_{ss}	Particle-wall restitution coefficient	0.60
ϕ	Specularity coefficient	0.60
Sc_t	Turbulent Schmidt number	0.90

Table 3 Comparison of the input parameters with predicted outlet values steady calculation (Huang et al., 2007)[16]

Parameters	Gas (kg/s)	Solid (kg/s)
Calculated (input inlet)	5.0372E-02	6.0517E-01
Simulation (outlet)	5.0463E-02	6.05141E-01
Imbalance (difference)	1.1078E-06	9.0682E-04
Fractional agreement	$\frac{1.1078E-06}{5.0463E-02}=2.0169E-05$	$\frac{9.0682E-04}{6.05141E-01}=0.001498$
% agreement	0.0020 %	0.1498%

Table 4 Comparison of the input parameters with predicted outlet values unsteady calculation) (Huang et al., 2007)

Parameters	Gas (kg/s)	Solid (kg/s)
Calculated (input inlet)	5.0372E-02	6.0517E-01
Simulation (outlet)	5.0463E-02	6.05141E-01
Imbalance (difference)	1.1081E-06	9.0795E-04
Fractional agreement	$\frac{1.1081E-06}{5.0463E-02}=2.1958E-05$	$\frac{9.0795E-04}{6.05141E-01}=0.0015$
% agreement	0.0022 %	0.1500%

The most essential factor is the application of the correct parameters, which is very importance in simulation of the gas-solid hydrodynamics for successful modelling of fluidised-bed riser reactor. The results presented in the above tables are steps toward achieving the targeted objectives in this study. Several grids were also put to dependency test, and were also established based on the comparisons of experimental data and modelling predictions of various grids, at various modelling conditions as shown below. After careful assessment with each of the grid, a resolution was arrived at using the grid size 565,520 cells, because the predictions were similar with grids 549,524 cells and 878,469 cells. Although, the grids sizes 565,520 cells and 549,524 cells are very close in size. However, due to simulation time-savings, there was no need using a large grid size 878,469 cells. In these independency tests, the grids 565,520 cells and 878,469 cells show a great overlap, but can easily be noticed clearly with the difference in colour coding.

For the CFX, to establish grid independency further, the predictions of solid holdup at radial position along the FCC riser height was carried out as shown in Figures 4 and 5. In each case, it is observed that, there are slight or not much differences between the grids sizes with 476,660 cells, 550,250 cells and 738,860 cells. These figures show the predictions comparison of the predictions with experimental data for three gas flow rates Case 1.1: 3.5 m/s and FCC solid loading of 100 kg/m^{2}s, Case 1.2: 5.5 m/s and FCC solid loading of 50

kg/m^{2}s, and Case 1.3: 5.5 m/s and FCC solid loading of 100 kg/m^{2}s at a radial position of x = 0.95 (r/R) for all these cases.

The grid size of 550,250 cells in CFX also provides sufficiently fine mesh size that give reasonable mesh independent results. For the Fluent, to establish the dependency test further in this case, the predictions of solid holdup at radial position along the FCC riser system were also carried out as shown in Figures 4 and 5. Figure 4 (a) represent Case 1.1, (b) for Case 1.2, and (c) for Case 1.3. In this case scenario, it was observed that, there were slight or no much observed differences between the grids sizes 549,524 cells, 565,520 cells and 878,469 cells.

The tests for restitution coefficient were equally carried out to further establish the grid dependency test. The detail effects of the restitution coefficient are shown in Figure 5. In this figure, a radial position of 0.95 were used to establish various effect of restitution coefficient with respect to gas-solid hydrodynamic flow along the FCC riser length. This study comparison was carried out for a straight FCC riser reactor.

4.1 Steady State Simulation of Straight FCC Riser using Fluent-Algebraic-KTGF and Comparison with CFX-algebraic-KTGF of Case 1.1.

With the effort to further study the prediction discrepancies found with the CFX simulations using algebraic-KTGF, we went ahead to study the hydrodynamic modelling of gas-solid in riser using ANSYS FLUENT solver, incorporating the algebraic-KTGF modelling approach. Figure 6 represent the particle velocity distribution and volume fractions in an FCC straight riser reactor, using algebraic-KTGF in Fluent solver.

In this Fluent steady state calculation, the simulation was run between iterations of 5000 – 8000 maximum, using automatic time scale control on a convergence target of 0.010 using realizable k-ε model, standard wall function, and second order resolution scheme.

A summary of the distribution profile are depicting the comparison of Fluent-algebraic-KTGF and CFX-algebraic-KTGF models are shown in Figures 7 and 8. Figure 7 represents the predictions of FCC velocity profile, while Figure 8 is representing the volume fraction along the riser reactor length. It is observed that, the main flow characteristics of the riser are better predicted by the Fluent solver (or software) modelling approach when compared with the previous (CFX) solver.

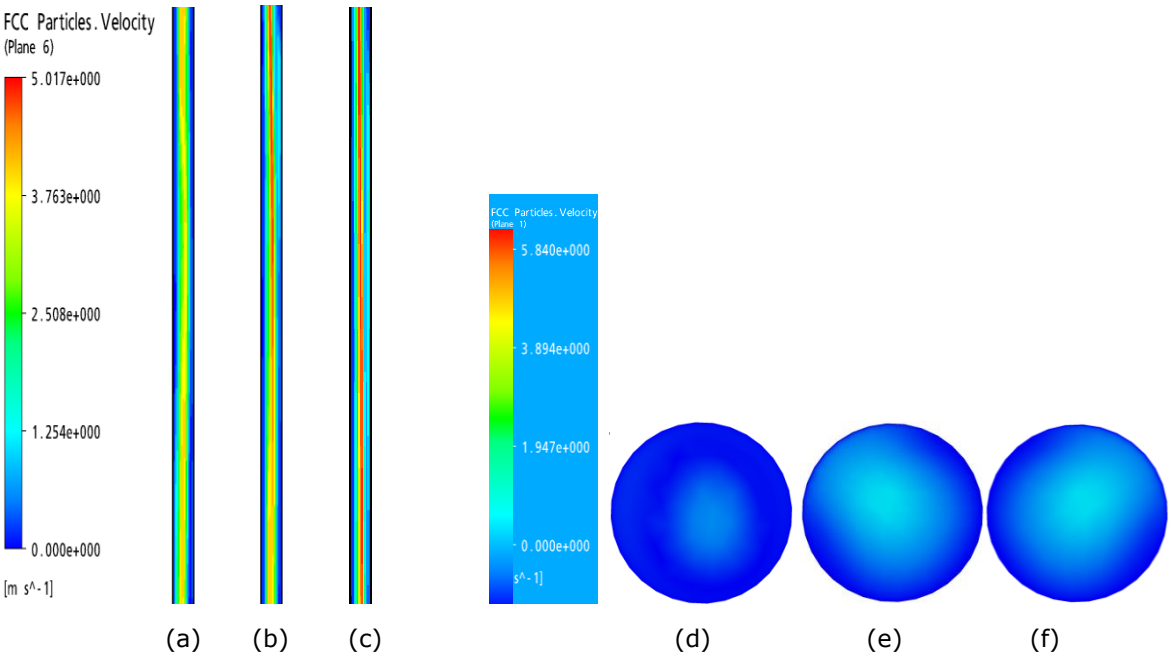

Fig 6: FCC profile distribution along a straight riser reactor: The velocity profile are (a) z = 0 – 0.95 m, (b) z = 0.95 m – 8.16 m and (c) z = 8.16 m – 14.08 m. While a 3-plane selection of the volume fraction are represented are at (d) z = 0.95 m, (e) z = 8.16 m and (f) z = 14.08 m. The grid size 565,520 cells were used, case 1.1 (Huang et al., 2007)

Both the solid flow velocity and volume fraction near the walls are generally well predicted better by this model, but still found in most cases to be less than the experimental values. These discrepancies in this case may be attributed to the simplifications used to reduce the computational difficulties of handling such complex and large system as reported previously by Makkawi and Ocone[18]. In addition, the assumption of modelling particles with mean size as monodispersed particles may attribute to these discrepancies. This approach could underestimate the agglomeration effect of large particles near the wall, which results in a lower solids concentration at the wall as predicted by this model. However, at z = 8.16 m, z = 10.0 m and z = 14.08 m, it was observed that the solid concentration is higher at the wall of the riser. They found that larger particles have more tendencies to accumulation near the wall than smaller ones. Although, the assumption of polydispersed particles in the modelling increases computational time, but can be a very useful option of addressing the multiphase hydrodynamic effect in fluidisation.

Conversely, it has been seen that the two solvers give a significant different results when using same boundary conditions and modelling approach. The reason for this may be due to method of discretisation techniques, which may differ in each of the two codes.

More so, the kinetic-collisional contribution in the solid stress tensor was considered, and this could possibly be another limitation to the predicted results. In addition, we found that with respect to straight riser and riser reactor with bend, the modelling predictions show some slight significant differences, although the prediction trends are similar. Refer to the appendix A1 of [5] for the details of the simulation of all other cases studied in this research work.

[18] Makkawi, Y, Ocone, R. (2006), *'A Model for Gas–Solid Flow in a Horizontal Duct with a Smooth Merge of Rapid–Intermediate–Dense Flows'*, Chemical Engineering Science **61**, pp. 4271 – 4281

Therefore, based on the modelling strategies adopted in this research work, it has made it a unique and outstanding approach in the study of gas-solid hydrodynamics, because this includes both the application of CFX and Fluent solver in the study. A base-case study was carried-out on case 1.1 using 3D geometry in CFX and Fluent solver. In the first instance, straight FCC riser reactor was used, which involve the steps as follows: (a) steady state non-KTGF (simple Miller Gidaspow) model, (b) steady state KTGF, and (c) algebraic-KTGF modelling approach. The predicted results from each of these steps were compared with reported data from literature.

In using the CFX-solver, it was found that with non-KTGF simulation [19],[20], the solver predictions were stable at low solid concentration and then at higher concentration, but was unstable when KTGF were included[21]. This characterise the ideal nature of gas-solid flow in the riser system. However, in CFX, it was difficult to capture the negative flow profile in the case study. Nevertheless, the CFX prediction trends give some reasonable when compared with reported data.

In the case of Fluent-CFD solver, there were tremendous improvement with respect to capturing recirculation, and negative downflow along the riser.

The validation of the fluent solver has proved better predictions when compared with CFX. Nevertheless, both solvers give reasonable predictions of gas-solid hydrodynamic flow in FCC riser.

In order to advance the study on gas-solid hydrodynamic, a more realistic approach of hydrodynamic study using transport-calculation were discussed in the subsequent sections. In the study, the predictions of pressure, FCC velocity and solid holdup etc., found in the study give a better agreement when compared with the experimental report. Since the straight FCC riser does not represent an ideal FCC riser, a challenge to model a real FCC riser arises. Therefore, the modelling of an FCC riser-bend, which may be a replica of an industrial riser, arises. However, it was noted that, the inclusion of bend-to-a straight riser has slight significance difference to the overall predictions observed in straight riser.

[19] Almuttahar, A. and Taghipour, F. (2007), *'Computational fluid dynamics of high density circulating fluidized bed riser: Study of modelling parameters'*, *Powder Technology*, **185**, pp. 11-23

[20] Makkawi, Y. and Ocone, R. (2007), 'Integration of ECT Measurements with Hydrodynamic Modelling of Conventional Gas-Solid Bubbling Bed', Chemical Engineering Science, pp. 4304 – 4315

[21] Makkawi, Y. and Ocone, R. (2005), 'Modelling of Particle Stress at the Dilute-Intermediate-Dense Flow Regimes: A review', KONA - Powder Science and Technology No.23, pp. 49 – 63, and Makkawi, Y., Wright, P. C. and Ocone, R. (2006), *'The Effect of Friction and Inter-Particle Cohesive Forces on the Hydrodynamics of Gas-Solid Flow: A Comparative Analysis of Theoretical Predictions and Experiments'*, Powder Technology **163**, pp. 69 – 79

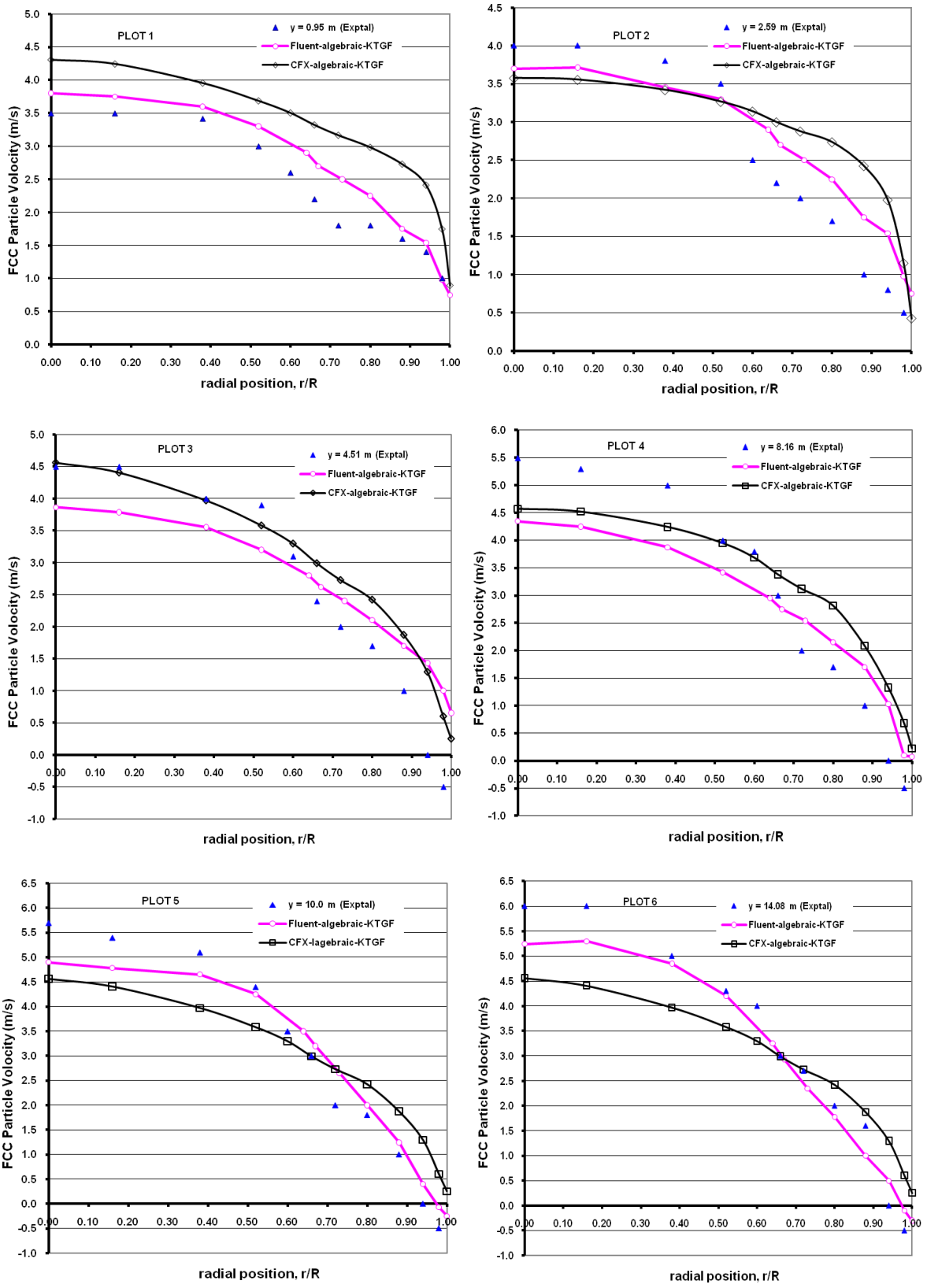

Figs 7: Radial profiles of FCC particle velocity along the FCC riser reactor (0.95 – 14.08 m). In Fluent solver the grid size used was 565,520 cells, while in CFX it was 550,250 cells used, case 1.1 (Huang et al., 2007)

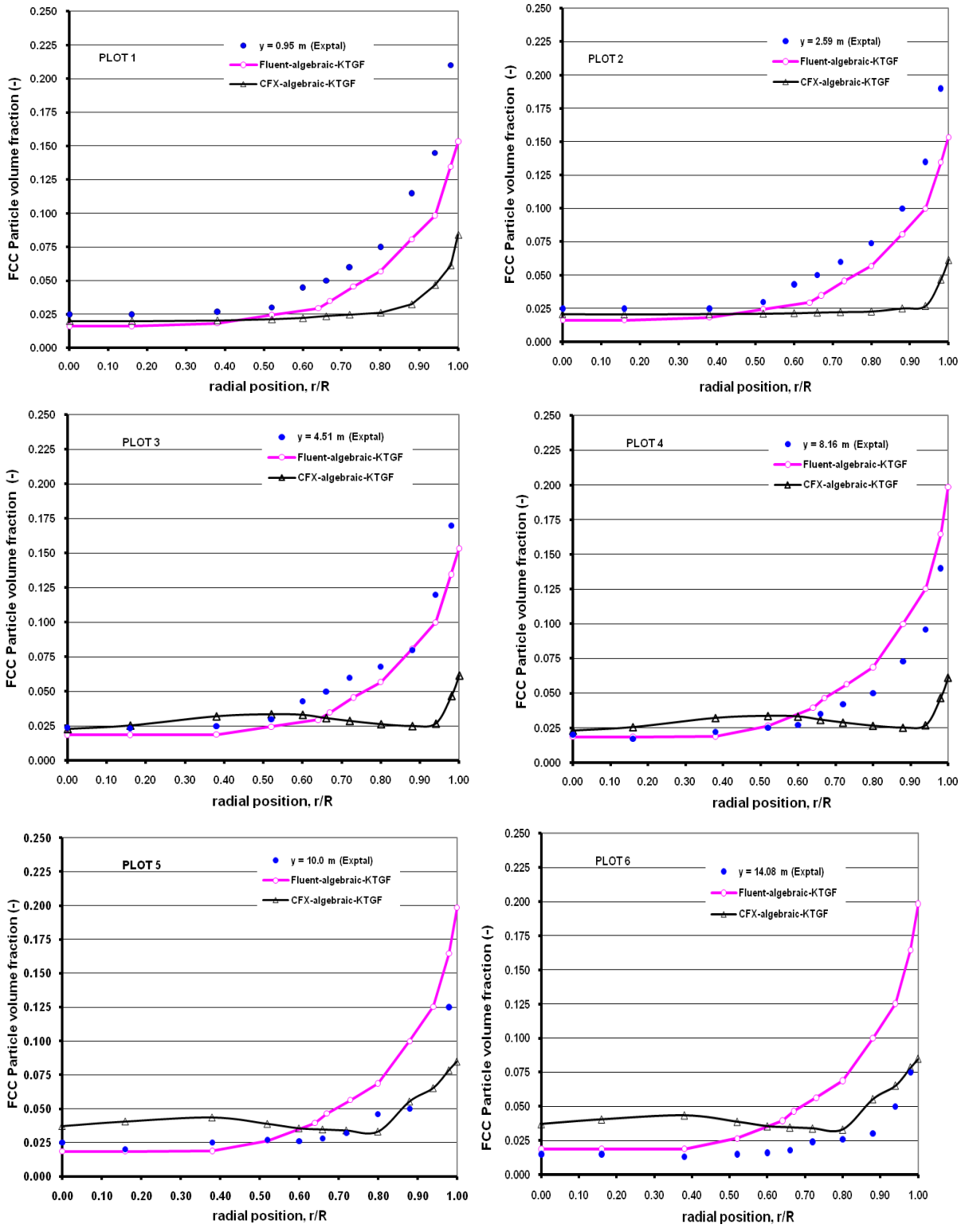

Figs 8: Radial profiles of FCC volume fraction along the FCC riser reactor (0.95 – 14.08 m) In Fluent solver the grid size used was 565,520 cells, while in CFX it was 550,250 cells used, case 1.1 (Huang et al., 2007).

5. Conclusion

Within the limit of the computational error, it was found that the choice of the ANSYS Fluent solver give the best approach to address the issue of gas-solid hydrodynamics in fluidised bed riser system of this kind, especially in the transient simulation condition of flow hydrodynamics.

In addition, the availability of transport KTGF in Fluent solver was a focus reason why the concluded choice of establishing a better understanding of the gas-solid hydrodynamics in riser reactors was arrived at. In summary, an adopted resolution of using a top-bend geometry configuration which fully represents a typical flow in FCC riser reactors to address the gas-FCC solid flow was used. Future studies to addressing a more robust CFD application are being considered more especially using ANSYS CFD 18.

Notations

A	Area m^2
c	Coefficient of Restitution
C	Courant number
D	Diameter
d_p	Particle diameter
$\bar{\varepsilon}_g$	Averaged voidage (volume fraction) in the reactor
$\bar{\varepsilon}_s$	Local solids holdup (volume fraction) in the FCC reactor
g	Acceleration due to gravity, 9.81 m/s^2
h	mesh spacing
L	Length of the riser pipe (m)
P	pressure (N/m^2)
Q_s	Heat flux between gas and solids phase, (J/s)
t	time, (s)
Δt	Time step (s)
t	Turbulent time scale
T	Temperature, (K)
$\vec{T}_s$	Stress tensors in solid medium
u_i	Mean velocity (m/s)
u'_i	Fluctuating velocity (m/s)
U_i	Instantaneous velocity (m/s)
ρ_g	Density of gas (Kg/m^3)
ρ_s	Density of solids catalyst (Kg/m^3)
μ	Gas viscosity, (Pa.s)
σ_k , σ_k , σ_ε	Constant
y_i	Weight fraction of component i
z	Axial position, (m)

Dimensionless Groups

$$\mathrm{Re} = \frac{\rho u D_i}{\mu} = \frac{u' L}{\nu}$$ Reynolds number standard

$$\mathrm{Pr} = \frac{\rho u l_i}{\mu}$$ Prandtl number

$$\mathrm{Re} = \frac{\rho_g d_s \left| \bar{v}_s - \bar{v}_g \right|}{\mu_g}$$ Reynolds number applied to gas-solid flow